Quantum dressed classical mechanics: Application to the photo-absorption of pyrazine

ARTICLE *in* CHEMICAL PHYSICS LETTERS · JANUARY 2003

Impact Factor: 1.9 · DOI: 10.1016/S0009-2614(02)01861-4

2 AUTHORS, INCLUDING:

Cecilia Coletti
Università degli Studi G. d'Annunzio C…

56 PUBLICATIONS **718** CITATIONS

Available online at www.sciencedirect.com
SCIENCE DIRECT®
Chemical Physics Letters 368 (2003) 289–298
CHEMICAL PHYSICS LETTERS
www.elsevier.com/locate/cplett

Quantum dressed classical mechanics: application to the photo-absorption of pyrazine

Cecilia Coletti [a], Gert D. Billing [b,*]

[a] *Dipartimento di Scienze del Farmaco, Universitá 'G. D'Annunzio', I-66100 Chieti, Italy*
[b] *Department of Chemistry, H. C. Ørsted Institute, University of Copenhagen, 2100 Ø Copenhagen, Denmark*

Received 25 September 2002; in final form 16 October 2002

Abstract

A newly formulated theory for treating time-dependent molecular quantum dynamics has been used to calculate the photo-absorption spectrum of pyrazine. Comparison with quantum mechanical results shows an excellent agreement during the whole propagation, proving that the present approach, when used in a discrete variable representation scheme, converges to exact quantum results if enough grid points are used. The addition of an increasing number of bath modes to the basic four mode model is also investigated and the performance of the method discussed.

1. Introduction

By expanding the wavefunction in a Gauss–Hermite (G–H) basis set, it is possible to parameterize the solution of the time-dependent Schrödinger equation in such a fashion that the equations of motion for some of the parameters appear as classical equations of motion, however with a potential which is more general than that known from ordinary Newtonian mechanics [1]. Together with the equations of motion of these parameters a set of equations in the expansion coefficients is obtained. Since the G–H basis set is complete one can proceed quite generally by applying ordinary Newtonian mechanics for the propagation of the above-mentioned parameters. In this manner it is possible to obtain a very convenient formulation, which is appealing from a computational point of view and which allows the blending of classical and quantum concepts in a new way. This scheme is especially convenient in the form in which a discrete variable representation (DVR) basis is introduced, avoiding the often cumbersome evaluation of matrix elements over basis functions and the potential. In this DVR formulation, the theory can be used near the classical limit with few grid points in a given degree of freedom or in the quantum limit with many grid points. Note that the one grid point limit corresponds to the classical limit. The method (also called quantum dressed classical mechanics) is not only easy to program, it is also efficient from a numerical point of view. In previous papers the

* Corresponding author. Fax: +45-35-320259.
E-mail addresses: ccoletti@unich.it (C. Coletti), gdb@theory.ki.ku.dk (G.D. Billing).

0009-2614/02/$ - see front matter
PII: S0009-2614(02)01861-4

time-dependent Gauss–Hermite DVR (TDGH-DVR) method has been used for treating inelastic scattering [2,3] and gas-phase [4,5] as well as surface reactions [6].

The theory is in this Letter used to compute the photo-absorption spectrum of pyrazine, using a model Hamiltonian developed in [7,8]. The investigation of pyrazine molecular dynamics after the photo-excitation to the S_2 electronic state has attracted much attention over the past years [7–13]. The characterization of its photo-absorption spectrum is extremely interesting both in order to reproduce the experimental results and from a methodological point of view.

2. Theory

We directly give the relevant equations of motion for the simplest but nevertheless completely general scheme which involves propagation of the DVR points using the classical equations of motion and a so-called fixed width approach for the basis set. For a derivation of these equations the reader is referred to [1,2,14,15]. The theory generates classical equations of motion for the center of the basis set or in the DVR representation the center of the DVR grid points. Thus, the grid points follow the classical equations of motion in space and if an odd number of grid points is used the middle one follows the classical trajectory. For a one-dimensional problem we therefore have the following equations of motion:

$$\dot{x}(t) = p_x(t)/m, \tag{1}$$

$$\dot{p}_x(t) = -\frac{\mathrm{d}V(x)}{\mathrm{d}x}|_{x=x(t)} \tag{2}$$

defining the trajectory, where m is the mass associated with the x-degree of freedom. In addition we get the following two equations describing the evolution in time of the width $A(t)$ and the phase $\gamma(t)$ of the Gaussian part of the Gauss–Hermite basis set:

$$\dot{A}(t) = -\frac{2}{m}A(t)^2 - \frac{1}{2}V''_{\mathrm{eff}}, \tag{3}$$

$$\dot{\gamma}(t) = \frac{p(t)^2}{m} + \mathrm{i}\hbar A(t)/m, \tag{4}$$

where V''_{eff} is an effective force. In the fixed-width approach $V''_{\mathrm{eff}} = 4\mathrm{Im}A(t)^2/m$.

For the quantum amplitudes we have the matrix equation

$$\mathrm{i}\hbar\dot{\mathbf{d}}(t) = (\mathbf{W}(t) + \mathbf{K})\mathbf{d}(t), \tag{5}$$

where $\mathbf{W}$ is a diagonal matrix and $\mathbf{K}$ the 'kinetic coupling' matrix. The elements of the kinetic matrix for a one-dimensional system are

$$K_{ij} = \frac{\hbar\alpha_0}{m}\sum_n \tilde{\phi}_n(z_i)(2n+1)\tilde{\phi}_n(z_j), \tag{6}$$

where α_0 is the imaginary part of the width parameter, i.e., $\alpha_0 = \mathrm{Im}A$ of the Gauss–Hermite basis set [1]. Since the kinetic operators have already worked on the basis functions before the DVR is introduced, the above matrix is what is left of the kinetic coupling. Eq. (5) are solved using a Split-Lanczos method [15]. Note that the kinetic energy matrix in coordinates weighted by $\sqrt{\alpha_0/m}$ is universal, i.e., independent on the system.

The zeros of the nth Hermite polynomial are denoted z_i and

$$\tilde{\phi}_n(z_i) = \phi_n(z_i)/\sqrt{A_i}, \tag{7}$$

$$A_i = \sum_n \phi_n(z_i)^2, \tag{8}$$

where

$$\phi_n(z) = \frac{1}{\sqrt{2^n n!\sqrt{\pi}}}\exp(-\frac{1}{2}z^2)H_n(z). \tag{9}$$

The elements of the diagonal matrix W are given as

$$W(x_i) = V(x_i) - V(x(t)) - \frac{\mathrm{d}V}{\mathrm{d}x}|_{x=x(t)}(x_i - x(t)) - \frac{2\alpha_0^2}{m}(x_i - x(t))^2, \tag{10}$$

i.e., the actual potential $V(x)$ minus a 'reference' potential defined by the forces evaluated at the trajectory. In the fixed width approach the second derivative is, as mentioned before, related to the imaginary part of the width and in the simplest possible approach the first derivative is taken as

the classical force in the sense of Newton. But we emphasize that more general forces may be applied [17,18,21]. The grid points follow the trajectory and are defined through

$$x_i = x(t) + \sqrt{\hbar/2\alpha_0}z_i. \tag{11}$$

Thus we can monitor the grid-density by varying the value of α_0. In the fixed width approach, the value of α_0 is kept constant and hence the grid points follow the trajectory $x(t)$ with constant distance. The above scheme is readily extended to any number of dimensions but in order to apply the method to pyrazine some modifications should be introduced.

3. The TDGH-DVR method for pyrazine

The experimental spectrum of pyrazine [19] consists of a broad band with little structure, sign of fast relaxation after the excitation, due to the existence of a conical intersection between the two excited states S_1 and S_2. This is by itself an element of interest, many molecular systems being described by non-adiabatic dynamics. The theoretical description of this spectrum, obtained by considering the main four vibrational modes, reproduces the essential dynamics of the system, but is not sufficient to obtain the experimental broad band, unless a Lorentzian broadening is inserted. The phenomenological dephasing constant required to reproduce the spectrum is such ($\tau = 30$ fs) that this broadening cannot be attributed to the spectrometer resolution only, but needs to be explained with the existence of a further ultrafast relaxation due to the interaction with the 20 remaining vibrational modes, affecting the dynamics as a weakly coupled heat bath. For this reason a model treating explicitly the bath degrees of freedom has to be introduced in order to describe the system dynamics in detail.

Recently a model Hamiltonian based on high level ab initio calculations [7,8], taking into account all the 24 modes of the system has been developed. Quantum benchmark calculations using the multiconfigurational time-dependent Hartree (MCTDH) method [20] have been carried out [7,8] giving a very good agreement with the experimental results and also providing for the possibility to test approximate methods. The richness (two electronic states, four vibrational modes, 20 bath modes) of such a model is indeed an optimal test for future applications of such schemes to very large and complex systems. In [13] a semiclassical approach has been used for this system, leading to fairly good results (a further discussion will be given in Section 4).

The application of the above-described TDGH-DVR approach to the pyrazine model introduced in [7] is straightforward and only few modifications are required.

The model Hamiltonian including the four main vibrational modes only is [7]

$$\begin{aligned} H = &\sum_i^4 \left(-\frac{\hbar^2}{2m}\frac{\partial^2}{\partial Q_i^2} + \frac{\omega_i^2 m}{2}Q_i^2 \right)\begin{pmatrix} 1 & 0 \\ 0 & 1 \end{pmatrix} \\ &+ \begin{pmatrix} -\Delta & 0 \\ 0 & \Delta \end{pmatrix} + \begin{pmatrix} 0 & \lambda \\ \lambda & 0 \end{pmatrix}\sqrt{\frac{m\omega_1}{\hbar}}Q_1 \\ &+ \sum_{j=2}^4 \begin{pmatrix} \kappa_j^{(1)} & 0 \\ 0 & \kappa_j^{(2)} \end{pmatrix}\sqrt{\frac{m\omega_j}{\hbar}}Q_j, \end{aligned} \tag{12}$$

where Q_is are the normal coordinates, among which Q_1 is, for symmetry reasons, the only mode which couples the two diabatic electronic states with off-diagonal matrix elements λ, i.e., the non-totally symmetric ν_{10a} mode; κ_is are the intrastate coupling constants for the remaining three tuning modes, which are totally symmetric ($\nu_1, \nu_{6a}, \nu_{9a}$). 2Δ is the energy gap between the two surfaces at the equilibrium condition ($\mathbf{Q} = \mathbf{0}$).

The Hamiltonian for the bath modes consists of a set of harmonic oscillators linearly coupled to the diabatic electronic states:

$$\begin{aligned} H_{\text{bath}} = \sum_i \Bigg[&\left(-\frac{\hbar^2}{2m}\frac{\partial^2}{\partial Q_i^2} + \frac{\omega_i^2 m}{2}Q_i^2 \right)\begin{pmatrix} 1 & 0 \\ 0 & 1 \end{pmatrix} \\ &+ \begin{pmatrix} \kappa_i^{(1)} & 0 \\ 0 & \kappa_i^{(2)} \end{pmatrix}\sqrt{\frac{m\omega_i}{\hbar}}Q_i \Bigg], \end{aligned} \tag{13}$$

where the sum is extended to the bath degrees of freedom taken into account. The first term in the sum represents the Hamiltonian for the bath itself, while the second describes the coupling between the system and the bath modes. The Hamiltonian

for the bath modes and for the normal tuning modes are formally identical, the only difference being the numerical values of the coupling constants: those corresponding to the bath modes are much weaker.

Inserting the above Hamiltonian into the time-dependent Schrödinger equation and utilizing the TDGH-DVR treatment we get the following equations for the first degree of freedom:

$$\dot{Q}_1(t) = \frac{p_1}{m}, \tag{14}$$

$$\dot{p}_1(t) = -\omega_1^2 m Q_1, \tag{15}$$

$$\dot{A}_1(t) = -\frac{2}{m}A_1(t)^2 - \frac{\omega_1^2 m}{2}, \tag{16}$$

$$\dot{\gamma}_1(t) = \frac{p_1^2(t)}{m} + i\hbar A_1(t)/m, \tag{17}$$

and for the others:

$$\dot{Q}_j(t) = \frac{p_j}{m}, \tag{18}$$

$$\dot{p}_j(t) = -\omega_j^2 m Q_j + \kappa_j^{(1)}\sqrt{\frac{m\omega_j}{\hbar}}, \tag{19}$$

$$\dot{A}_j(t) = -\frac{2}{m}A_j(t)^2 - \frac{\omega_j^2 m}{2}, \tag{20}$$

$$\dot{\gamma}_j(t) = \frac{p_j^2(t)}{m} + i\hbar A_j(t)/m, \tag{21}$$

which are analogous to Eqs. (1)–(4). The last four equations have the same form for the vibrational normal modes and for the bath modes. Eqs. (14)–(21) have been obtained by letting the trajectory which carries the DVR points propagate on one of the surfaces only, namely the lower one, however the final result should be independent on the surface choice. The trajectory is thus driven by the effective force which can be taken as the derivative of the adiabatic lower potential, that is we have

$$V_{\text{clas}}(\mathbf{Q}(t)) = \sum_i \frac{\omega_i m Q_i^2(t)}{2} + \sum_{j>2}\kappa_j^{(1)}\sqrt{\frac{m\omega_j}{\hbar}}Q_j(t) - \Delta.$$

The DVR grid points will follow the classical trajectory in time; the position of the grid point n for the ith degree of freedom is given by

$$Q_{i,n} = Q_i(t) + \sqrt{\frac{\hbar}{2\mathrm{Im}A_i(t)}}z_n \tag{22}$$

(see also Eq. (11)).

The differential equation for the quantum amplitudes (i.e., the generalisation of Eq. (5)) for the grid point nm is given by (we consider here only two degrees of freedom for simplicity)

$$\begin{aligned} i\hbar\begin{pmatrix}\dot{d}_{nm}^{(1)}\\ \dot{d}_{nm}^{(2)}\end{pmatrix} &= \begin{pmatrix}0 & W_{nm;n'm'}^{(12)}\\ W_{nm;n'm'}^{(12)} & W_{nm;n'm'}^{(22)}\end{pmatrix}\begin{pmatrix}d_{nm}^{(1)}\\ d_{nm}^{(2)}\end{pmatrix}\delta_{nn'}\delta_{mm'}\\ &+ \frac{\hbar\mathrm{Im}A_1}{m}\delta_{mm'}\begin{pmatrix}\sum_{k=1}^{N_1}K_{nk}d_{km}^{(1)}\\ \sum_{k=1}^{N_1}K_{nk}d_{km}^{(2)}\end{pmatrix}\\ &+ \frac{\hbar\mathrm{Im}A_2}{m}\delta_{nn'}\begin{pmatrix}\sum_{k=1}^{N_2}K_{mk}d_{nk}^{(1)}\\ \sum_{k=1}^{N_2}K_{mk}d_{nk}^{(2)}\end{pmatrix}, \end{aligned} \tag{23}$$

where $d_{nm}^{(1)}$ stands for d_{nm} on the first surface and N_1 and N_2 are the number of grid points used in the first and second degrees of freedom, respectively. K_{nk} and K_{mk} are the generic elements of the kinetic energy matrix (Eq. (6)) coupling the grid points in the first and the second degrees of freedom, respectively. $\mathbf{W}_{nm;n'm'}$ are the elements of the potential coupling, which can be obtained as in Eq. (10)

$$W_{nm;nm}^{(12)} = \lambda\sqrt{\frac{\omega_1 m}{\hbar}}Q_{1,n}, \tag{24}$$

$$W_{nm;nm}^{(22)} = \sum_{j>1}\left(\kappa_j^{(2)} - \kappa_j^{(1)}\right)\sqrt{\frac{\omega_m m}{\hbar}}Q_{j,m} + 2\Delta \tag{25}$$

(holding also for more than two degrees of freedom). Thus the two states are coupled by a 2×2 matrix at each grid point, provided that the grid points on the two surfaces are the same. This can be obtained by letting the trajectory which carries the DVR points propagate on one of the surfaces only.

In order to solve Eq. (23) using the same Lanczos scheme as for single surface problems the vector $\mathbf{d}$ has to be transformed in such a way that the potential $\mathbf{W}_{nm}$ becomes diagonal. A transformation matrix $\mathbf{C}$ is defined such that

$$\mathbf{C}_{nm}^{-1}\mathbf{W}_{nm}\mathbf{C}_{nm} = \begin{pmatrix}\overline{\mathbf{W}}_{nm;n'm'}^{(1)} & 0\\ 0 & \overline{\mathbf{W}}_{nm;n'm'}^{(2)}\end{pmatrix}. \tag{26}$$

If we now introduce

$$\begin{pmatrix} e_{ij}^{(1)} \\ e_{ij}^{(2)} \end{pmatrix} = \mathbf{C}_{ij}^{-1} \begin{pmatrix} d_{ij}^{(1)} \\ d_{ij}^{(2)} \end{pmatrix} \tag{27}$$

and apply the above orthogonal transformation to the set of Eq. (23), we get:

$$\begin{aligned} \mathrm{i}\hbar \begin{pmatrix} \dot{e}_{nm}^{(1)} \\ \dot{e}_{nm}^{(2)} \end{pmatrix} &= \begin{pmatrix} \overline{W}^{(1)}_{nm;n'm'} & 0 \\ 0 & \overline{W}^{(2)}_{nm;n'm'} \end{pmatrix} \begin{pmatrix} e_{nm}^{(1)} \\ e_{nm}^{(2)} \end{pmatrix} \delta_{nn'}\delta_{mm'} \\ &+ \frac{\hbar \mathrm{Im}A_1}{m} \delta_{mm'} \mathbf{C}^{-1}_{nm} \begin{pmatrix} \sum_{k=1}^{N_1} K_{nk} d_{km}^{(1)} \\ \sum_{k=1}^{N_1} K_{nk} d_{km}^{(1)} \end{pmatrix} \\ &+ \frac{\hbar \mathrm{Im}A_2}{m} \delta_{nn'} \mathbf{C}^{-1}_{nm} \begin{pmatrix} \sum_{k=1}^{N_2} K_{mk} d_{nk}^{(1)} \\ \sum_{k=1}^{N_2} K_{mk} d_{nk}^{(2)} \end{pmatrix}. \end{aligned} \tag{28}$$

These equations can then be propagated by the Lanczos method one time-step to get $\mathbf{e}(t+\Delta t)$ from which $\mathbf{d}(t+\Delta t)$ can be obtained using the inverse transformation. Eq. (28) is more complex than that obtained for a multisurface problem involving only one degree of freedom (see for example Eq. (30) of [16]), which can be expressed in a compact form as a function of the vector **e** only. In the present case, due to the summations in the last two terms of Eq. (28) (which are absent in the one degree of freedom derivation), for each grid point *nm* the sum over the components of the original **d** vector has to be transformed by $\mathbf{C}^{-1}_{nm}$. This has to be taken into account inside the Lanczos propagation.

The wavefunction is initialized on the surface S_2 and is taken as a product of harmonic oscillators in their ground state $h_0(x_i)$

$$\Psi^{(2)}_{t_0} = \prod_i^{N_2} h_0(Q_i(t_0)) \tag{29}$$

whereas the wavefunction on surface S_1 is

$$\Psi^{(1)}_{t_0} = 0. \tag{30}$$

To have the initial expansion coefficients $\mathbf{d}(t_0)$ we need to project the initial wavefunction (29) onto the G–H basis set (again in the case of two degrees of freedom only)

$$d^{(1)}_{nm}(t_0) = 0, \tag{31}$$

$$\begin{aligned} d^{(2)}_{nm}(t_0) = &\left(\frac{\hbar}{2\mathrm{Im}A_1(t_0)}\right)^{1/4} \left(\frac{\hbar}{2\mathrm{Im}A_2(t_0)}\right)^{1/4} \\ &\times \exp\left(\gamma_1(t_0) + \frac{\mathrm{i}}{\hbar}[p_1(t_0)(Q_{1,n} - Q_1(t_0)) \right. \\ &\left. + \mathrm{Re}A_1(t_0)(Q_{1,n} - Q_1(t_0))^2]\right) \\ &\times \exp\left(\gamma_2(t_0) + \frac{\mathrm{i}}{\hbar}[p_2(t_0)(Q_{2,m} - Q_2(t_0)) \right. \\ &\left. + \mathrm{Re}A_2(t_0)(Q_{2,m} - Q_2(t_0))^2]\right) \\ &\times \frac{1}{\sqrt{A_1 A_2}} h_0(Q_1(t_0)) h_0(Q_2(t_0)), \end{aligned} \tag{32}$$

where the A_is are given by Eq. (8).

The dynamical evolution of the system in time is thus studied by simultaneously propagating Eqs. (14)–(21) and the set of differential equations (28). The accuracy of the integration procedure can be verified by monitoring the conservation of the wavefunction norm. The population on the two surfaces at the generic time t can be obtained directly from the vectors

$$\begin{pmatrix} \mathbf{d}^{(1)}(t) \\ \mathbf{d}^{(2)}(t) \end{pmatrix},$$

since it can be shown [2] that $|d^{(k)}_{nm}|^2$ represents the probability for being on the surface (k) at the grid point n in the first normal mode and at the point m in the second normal mode. Thus the probability for the system of being on the surface S_2 at the time t is given by a simple 'grid summation'

$$P^{(2)}(t) = \sum_{nm}^{N_1 N_2} |d^{(2)}_{nm}|^2. \tag{33}$$

4. Results

The photo-absorption spectrum of pyrazine can be obtained from the Fourier transform of the autocorrelation function $C(t)$

$$I(\omega) = \omega \int_{-\infty}^{\infty} C(t)\, \mathrm{e}^{\mathrm{i}\omega t}\, \mathrm{d}t, \tag{34}$$

where

$$C(t) = \langle \Psi(t) | \Psi(0) \rangle = \left\langle \Psi^*\left(\frac{t}{2}\right) \middle| \Psi\left(\frac{t}{2}\right) \right\rangle. \tag{35}$$

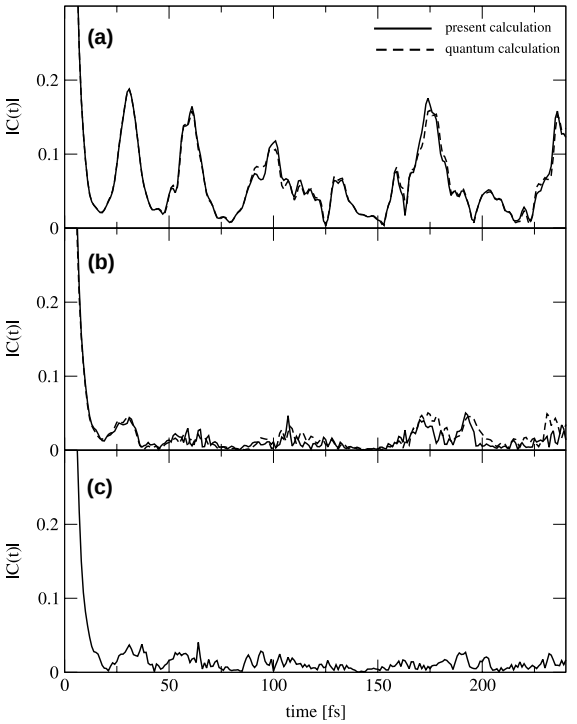

Fig. 1. Modulus of the autocorrelation function (Eq. (35)) $C(t)$ as a function of propagation time for the four mode model (a) employing 22, 29, 17 and 13 grid points in each mode and with the inclusion of five (b) and 10 (c) bath modes. Comparison between the present TDGH-DVR calculation (solid line) and exact quantum results [7] (dashed line) is also shown. The calculation of panel b was performed using 17, 27 13 and 9 points for the four main modes and 1, 4, 1, 3 and 3, respectively, for the bath modes – the order in the inclusion of the vibrational modes is the same of Table 1 in [7], while for panel c 17, 18, 9, 6 points in the main and 1, 3, 1, 3, 3, 2, 2, 1, 1, 1 in the bath modes were used.

The latter part of this expression has been employed since it has been demonstrated [22] that it is both faster and more accurate. It holds if the initial wavefunction is real and the Hamiltonian symmetric.

In order to avoid artifacts in the spectrum (the Gibbs phenomenon), due to the finite time of the propagation, prior to the spectrum calculation the autocorrelation function is multiplied by a factor

$$g(t) = \cos\left(\frac{\pi t}{2T}\right), \tag{36}$$

where T is the total propagation time, so that $C(t)$ is brought smoothly to zero.

The numerical values of the parameters of the Hamiltonian (Eqs. 12 and 13), unless otherwise specified, have been taken from [7].

In the following the modulus of the autocorrelation function, the diabatic population of the surface S_2 and the spectrum calculated with the method just described will be reported using first the four vibrational main modes only and then when an increasing number of bath degrees of freedom is added. The exact quantum results of [7] will also be reported for comparison.

A propagation time of 120 fs (corresponding to a $T = 240$ fs in the propagation of the autocorrelation function) and a time-step of 0.5 fs have been used in each of the following models.

4.1. Four mode model

The autocorrelation function (Eq. 35) for the system has been calculated using 22 DVR grid points in the first mode (i.e., the coupling mode ν_{10a}) and 29, 17 and 13 grid points respectively for the other tuning modes ($\nu_1, \nu_{6a}, \nu_{9a}$).

We used the following initial values for the coordinates, momenta, widths and phases of the G–H wavepacket:

$$\begin{aligned} Q_i(t_0) &= 0, \\ p_i(t_0) &= \sqrt{\hbar\omega_i}, \\ \mathrm{Re}A_i(t_0) &= 0, \\ \mathrm{Im}A_i(t_0) &= \frac{1}{2}m\omega_i, \\ \mathrm{Re}\gamma_i(t_0) &= 0, \\ \mathrm{Im}\gamma_i(t_0) &= -\frac{\hbar}{4}\log\left(\frac{2\mathrm{Im}A_i(t_0)}{\pi\hbar}\right). \end{aligned} \tag{37}$$

The initial value of the classical momentum is not crucial (for example it can be taken equal to zero) the quantum result being independent on the initial choice, provided that a sufficient number of grid points is used, but this choice becomes important when very few points are used, in particular in the limit of a single grid point, since in that case the dynamics of the system is completely governed by classical mechanics.

The modulus of the autocorrelation function as a function of propagation time is shown in Fig. 1a

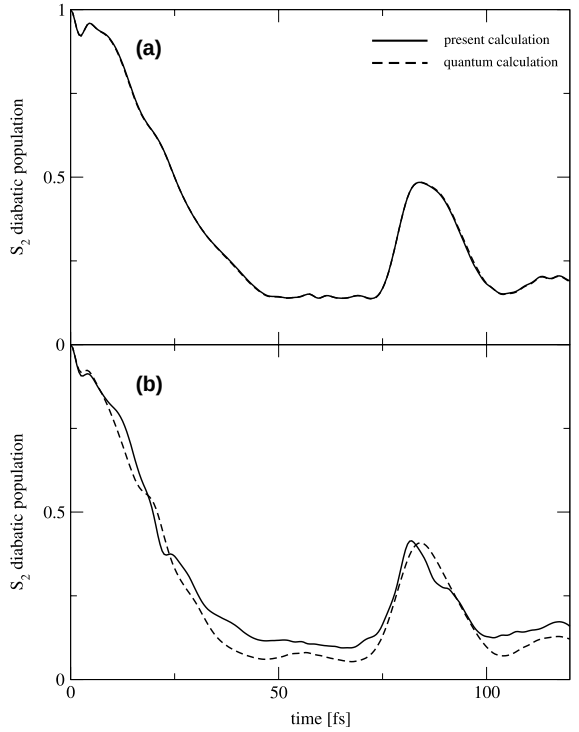

Fig. 2. S_2 diabatic population as a function of propagation time for the four mode model (a) and with the inclusion of five (b) bath modes. Comparison between the present TDGH-DVR calculation (solid line) and exact quantum results [7] (dashed line) is shown.

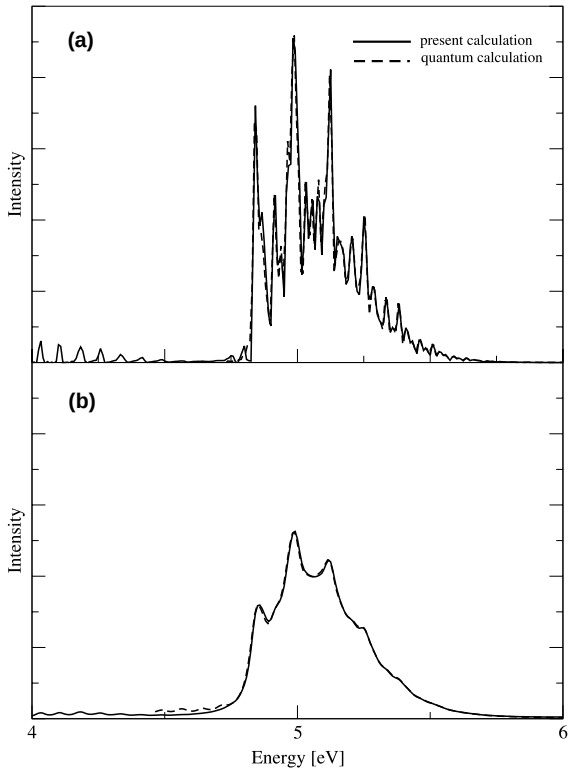

Fig. 3. Pyrazine photo-absorption spectrum for the four mode model of Section 4.1. In (b) an artificial phenomenological broadening was taken into account (by means of a dephasing constant $\tau = 30$ fs). (Present work – solid line, quantum result [7] – dashed line).

together with the quantum results for the same four mode system.

The agreement with the quantum results is excellent: the first peak is identical in the two approaches, and only very small differences appear for the other resonances. It is remarkable that this behaviour is maintained throughout the whole propagation: there is not a loss of coherence, as it happens, for instance, for the semiclassical method used in [13], which, although reproducing rather well the quantum autocorrelation function for a propagation time less than 80 fs, leads to very large deviations at longer times.

The fact that our calculations nearly coincide with the quantum ones is a confirmation that the TDGH-DVR method fully converges to the exact quantum mechanical results if a sufficiently large number of grid points is utilized. The small deviations shown in Fig. 1a can be eliminated by adding more points in the grid. However, also in view of increasing the number of modes explicitly included in the model and thus the related number of grid points, Fig. 1a shows that, even with a moderate number, the present calculation leads to a result very close to the quantum one. The same trend of Fig. 1a can be seen in Fig. 2a and Fig. 3.

Fig. 2a shows the population of the diabatic electronic state S_2, which is linked to the coupling of the diabatic states and thus to the effect of the conical intersection. In this case the line representing the quantum results perfectly coincides with our calculation. In Fig. 3 the pyrazine absorption spectrum is reported for the same four-mode model, in panel (b) of the same figure the spectrum is obtained with the inclusion of the phenomenological broadening enabling the com-

parison with the experiments. In both cases – (a) and (b) – the agreement with the quantum results is extremely good.

The computational effort for this calculation is rather small, requiring a memory of 99 MBytes and 54.7 min of CPU time on a PC, using a Pentium III 1000 MHz processor. Although the CPU time for the MCTDH calculation (performed on a IBM RS/6000 power 2 workstation) is even smaller it must be stressed that in the present case no considerations about the symmetry of the system or grouping of the modes were made. The comparison with the numerical effort of the semiclassical calculations of [13], performed on a COMPAQ XP1000 workstation (15 CPU hours and $\approx$4 MBytes of memory) also shows that the present method is very competitive in terms of required computational time.

4.2. System + bath modes

The effect of the inclusion of the bath modes has been studied by considering an increasing number of bath degrees of freedom in the calculation starting from those more strongly coupled.

The analysis of the results illustrated above and the consideration that the Hamiltonian for the bath modes is formally identical to that for the three tuning modes leads to the conclusion that with enough grid points it is possible to reproduce the exact quantum results. Since the calculation has been carried out on a PC computer only a limited number of total DVR grid points could be taken into account, as it will be discussed in the following. In particular for the five bath modes case a maximum of 2 million points on each surface could be considered and thus a compromise had to be reached between the number of grid points for the principal normal modes and those for the bath modes. Since these are more weakly coupled a smaller number of grid points will be necessary to describe them.

Figs. 1b, 2b and 4 have thus been obtained by explicitly considering five bath modes beside the four nuclear ones. The modulus of the autocorrelation function for such a system is reported in Fig. 1b. Although the number of grid points (explicitly reported in the figure captions) for the nuclear modes has been diminished the agreement with the quantum results is still good: the position of the recurrences is the same and the quantitative agreement is very good for the first peak and becomes only slightly worse as the propagation time increases. There is a strong damping in the peak intensity with respect to Fig. 1b, connected to the presence of the bath modes. This is also shown in Fig. 2b depicting the diabatic population of S_2 electronic state: a faster depopulation compared to Fig. 2a is clearly seen, even if not so strong as in the quantum calculation. Fig. 4 shows the photo-absorption spectrum. The inclusion of the bath modes provides for a broader and less structured spectrum similar to that of Fig. 3b which was obtained by the four mode model with the addition of a phenomenological broadening in order to reproduce the experimental results. Comparison with the quantum calculation shows that the magnitude of the broadening is well reproduced although some details in the structure are missing, most likely due to the decrease in the number of points used for the description of the four main modes.

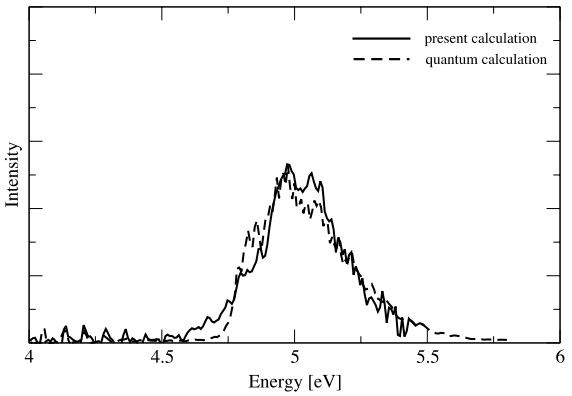

Fig. 4. Pyrazine photo-absorption spectrum for the four mode model + five bath modes of Section 4.2. (Present work – solid line, quantum result [7] – dashed line).

On the computational effort side the increase in the number of grid points increases memory and CPU time requirements: the Lanczos propagation scheme requires all the recursion vectors to be stored, writing them to the disk can limit the memory load, but the I/O will increase the com-

putational time. As an example the four mode calculation described in Section 4.1 would now require 56 MBytes and 201 min of CPU time. Thus for the calculation involving the system + five bath modes a CPU time of 3236 min and a memory of 924 MBytes were required.

The inclusion of five additional bath modes was also tested: a calculation where a single point was used in each of the new degrees of freedom did not lead to a sufficiently effective relaxation, proving that a quantum treatment was needed at least for those modes having the largest coupling constants κ. For the reason illustrated above in order to perform such a test we had to further reduce the number of grid points in the main modes, so to have a computational cost comparable with the previous calculation.

The corresponding autocorrelation function is reported in Fig. 1c where a further damping in the peak intensity is shown; the last two panels of Fig. 1 thus show that even if only few points have been employed for the description of the bath modes the overall agreement with the quantum behaviour is very good.

5. Conclusions

In this work we have applied the TDGH-DVR method to a multi-surface, many degrees of freedom problem such as the calculation of the pyrazine photo-absorption spectrum. This treatment is completely general and does not depend on the form of the Hamiltonian employed, as it happens, for example in the MCTDH formalism where the exact quantum results could be obtained thanks to the simplicity of the model and to symmetry considerations. The method, thanks to its flexibility, is very easy to implement, even for complex systems characterized by different features. For instance the solution of the set of Eq. (28), although looking much more complicated than the single-surface, single degree of freedom counterpart, in fact – except for the mentioned small modification on the Lanczos propagation procedure – only requires the addition of some sums and 'do-loops' to the original code, leaving its basic structure unchanged.

It has been shown, as in the four mode model, that with enough grid points the method converges to a quantum mechanical description and the computational load is rather limited compared to usual DVR approaches. The introduction of additional bath degrees of freedom requires a larger computational effort, however it can still be dealt with when the coupling to the system is weak so that they can be described with very few grid points. The agreement with the quantum results is still rather good.

In the limit of a single grid point, i.e., when a classical description is employed – for example for those modes which are only very weakly coupled to the system – the computational load remains practically unchanged, although the additional degrees of freedom are explicitly taken into account. This opens up an appealing perspective for the application of such a scheme, possibly in combination with direct dynamics methods, to the description of quantum mechanical phenomena taking place in a restricted region of large systems, like proton transfer in biological reactions [23].

Acknowledgements

This research is supported by the Carlsberg Science Foundation and the EU-TMR Grant: HPRN-CT-1999-00005. Dr. Graham Worth is acknowledged for providing us with the exact quantum data.

References

[1] G.D. Billing, J. Chem. Phys. 114 (2001) 6641.
[2] G.D. Billing, S. Adhikari, Chem. Phys. Lett. 197 (2000) 34.
[3] G.D. Billing, Chem. Phys. 264 (2001) 71.
[4] G.D. Billing, Int. J. Quantum Chem. 84 (2001) 467.
[5] C. Coletti, G.D. Billing, Chem. Phys. Lett. 264 (2001) 61.
[6] G.D. Billing, J. Phys. Chem. A 105 (2001) 2340.
[7] G.A. Worth, H.D. Meyer, L.S. Cederbaum, J. Chem. Phys. 109 (1998) 3518.
[8] A. Raab, G.A. Worth, H.D. Meyer, L.S. Cederbaum, J. Chem. Phys. 110 (1999) 936.
[9] G.A. Worth, H.D. Meyer, L.S. Cederbaum, Chem. Phys. Lett. 299 (1999) 451.
[10] C. Woywood, W. Domcke, A.L. Sobolewski, H.-J. Werner, J. Chem. Phys. 100 (1994) 1400.

[11] S. Krempl, M. Winterstetter, H. Plöhn, W. Domcke, J. Chem. Phys. 100 (1994) 926.
[12] G.A. Worth, H.D. Meyer, L.S. Cederbaum, J. Chem. Phys. 105 (1996) 4412.
[13] M. Thoss, W.H. Miller, G. Stock, J. Chem. Phys. 112 (2000) 10282.
[14] G.D. Billing, Phys. Chem. Chem. Phys. 4 (2002) 2865.
[15] G.D. Billing, Chem. Phys. Lett. 237 (2001) 339.
[16] G.D. Billing, Chem. Phys. Lett. 343 (2001) 130.
[17] G.D. Billing, J. Chem. Phys. 107 (1997) 4286.
[18] G.D. Billing, J. Chem. Phys. 111 (1999) 48.
[19] I. Yamazaki, T. Murao, T. Yamanaka, K. Yoshihara, Faraday Discuss. 75 (1983) 395.
[20] See, for example, H.D. Meyer, in: P. von Schleyer (Ed.), Encyclopedia of Computational Chemistry, Wiley, New York, 1998.
[21] G.D. Billing, in: A. Laganá, A. Riganelli (Eds.), Reaction and Molecular Dynamics, Lecture Notes in Chemistry, 75, Springer, Berlin, 2000, p. 115.
[22] V. Engel, Chem. Phys. Lett. 189 (1992) 76.
[23] C. Coletti, F. de Angelis, N. Re, G.D. Billing, work in progress.